bioRxiv preprint doi: https://doi.org/10.1101/856864; this version posted November 27, 2019. The copyright holder for this preprint (which was not certified by peer review) is the author/funder, who has granted bioRxiv a license to display the preprint in perpetuity. It is made available under aCC-BY 4.0 International license.

1 # *ALTERED MERISTEM PROGRAM1* regulates leaf identity independent of miR156-
2 mediated translational repression

3

4 **Running title: *AMP1* and vegetative phase change**

5

6 Jim P. Fouracre, Victoria J. Chen and R. Scott Poethig*

7

8 Biology Department, University of Pennsylvania, 433 S. University Ave, Philadelphia,
9 Pennsylvania, 19104, USA

10

11 Corresponding author: Poethig, R. S. (spoethig@sas.upenn.edu)

12

13

14 **Keywords**
15 Vegetative phase change, shoot apical meristem, miR156, *SPL*, *AMP1*, translational
16 repression

17

18

19 **Summary statement**
20 We show that loss of the carboxypeptidase, AMP1, does not interfere with the function
21 of miR156 or miR159, suggesting that AMP1 is not universally required for miRNA-
22 mediated translational repression in *Arabidopsis*.

23

bioRxiv preprint doi: https://doi.org/10.1101/856864; this version posted November 27, 2019. The copyright holder for this preprint (which was not certified by peer review) is the author/funder, who has granted bioRxiv a license to display the preprint in perpetuity. It is made available under aCC-BY 4.0 International license.

24 **Abstract**

25 In *Arabidopsis*, loss of the carboxypeptidase, ALTERED MERISTEM PROGRAM1
26 (AMP1), produces an increase in the rate of leaf initiation, an enlarged shoot apical
27 meristem and an increase in the number of juvenile leaves. This phenotype is also
28 observed in plants with reduced levels of miR156-targeted *SQUAMOSA PROMOTER*
29 *BINDING PROTEIN-LIKE* (*SPL*) transcription factors, suggesting that AMP1 may
30 promote SPL activity. However, we found that the *amp1* phenotype is only partially
31 corrected by elevated *SPL* gene expression, and that *amp1* has no significant effect on
32 *SPL* transcript levels, or on the level or the activity of miR156. Although evidence from
33 a previous study suggests that AMP1 promotes miRNA-mediated translational
34 repression, *amp1* did not prevent the translational repression of the miR156 target,
35 *SPL9,* or the miR159 target, *MYB33.* These results suggest that *AMP1* regulates
36 vegetative phase change downstream of, or in parallel to, the miR156/*SPL* pathway and
37 that it is not universally required for miRNA-mediated translational repression.

38

39

40

41

42

43

bioRxiv preprint doi: https://doi.org/10.1101/856864; this version posted November 27, 2019. The copyright holder for this preprint (which was not certified by peer review) is the author/funder, who has granted bioRxiv a license to display the preprint in perpetuity. It is made available under aCC-BY 4.0 International license.

44 **INTRODUCTION**

45 Plant life-histories are underpinned by a series of developmental transitions, the correct
46 timing of which are crucial to plant survival and reproductive success (Huijser and
47 Schmid, 2011). Vegetative phase change describes the switch between the juvenile and
48 adult stages of vegetative growth. Depending on the species, this transition can lead to
49 shifts in a wide variety traits (Poethig, 2013). In the model plant, *Arabidopsis thaliana*,
50 the juvenile vegetative phase is associated with small, round leaves that lack both
51 trichomes on the abaxial leaf surface and serrations, whereas the adult phase is
52 characterized by larger, elongated and serrated leaves that produce abaxial trichomes.

53 The core genetic network that controls the timing of vegetative phase change has
54 been well described. The microRNA miR156, and its sister miR157, function as master
55 regulators of the juvenile phase. A temporal decline in miR156/miR157 during shoot
56 development leads to an increase in expression of their target genes—*SQUAMOSA*
57 *PROMOTER BINDING PROTEIN-LIKE* (*SPL*) transcription factors—which promote the
58 adult phase (Wu and Poethig, 2006; Wu et al., 2009). This temporal mechanism is
59 widely conserved and regulates shoot identity in diverse plant lineages (Chuck et al.,
60 2007; Leichty and Poethig, 2019; Riese et al., 2008; Wang et al., 2011). *SPL* genes are
61 known to promote the expression of miR172, which initiates adult development through
62 repression of its targets in the *APETALA2-LIKE* (*AP2-LIKE*) gene family. Vegetative
63 phase change is thus promoted by inverse gradients of expression of two miRNAs,
64 miR156 and miR172 (Wu et al., 2009).

65 *ALTERED MERISTEM PROGRAM1* (*AMP1*), which encodes a putative
66 carboxypeptidase (Helliwell et al., 2001), was identified in a genetic screen for phase

bioRxiv preprint doi: https://doi.org/10.1101/856864; this version posted November 27, 2019. The copyright holder for this preprint (which was not certified by peer review) is the author/funder, who has granted bioRxiv a license to display the preprint in perpetuity. It is made available under aCC-BY 4.0 International license.

67 change mutations over 20 years ago (Conway and Poethig, 1997), but the basis for its
68 effect on this process is still unknown. Mutations in *AMP1* produce a large number of
69 small, round leaves that lack abaxial trichomes (juvenile leaves) and have a higher rate
70 of leaf initiation (Telfer et al., 1997). An initial study suggested that this phenotype was
71 not associated with a change in the timing of vegetative phase change, leading to the
72 conclusion that the timing of vegetative phase change is regulated independently of
73 leaf number (Telfer et al., 1997). However, this result conflicts with more recent studies
74 showing that pre-existing leaves promote vegetative phase change (Yang et al., 2011;
75 Yang et al., 2013; Yu et al., 2013). The phenotype of *amp1* is also surprising given the
76 evidence that AMP1 is required for miRNA-mediated translational repression (Li et al.,
77 2013). miR156 promotes juvenile development by translationally repressing its targets
78 (He et al., 2018). If AMP1 is required for miRNA-mediated translational repression,
79 *amp1* mutants would therefore be expected to have to a reduced number of juvenile
80 leaves due to elevated *SPL* gene expression, which is the exact opposite of the *amp1*
81 phenotype.
82 To resolve these issues, we investigated the interaction between *AMP1* and the
83 miR156-*SPL* module. Our results indicate that *AMP1* promotes adult leaf traits in
84 parallel to, or downstream of, the miR156-*SPL* module. We also found no evidence that
85 AMP1 is required for translational repression by either miR156 or miR159. This latter
86 result suggests that the mechanism by which miRNAs repress translation in plants is
87 different for different transcripts.
88
89 **RESULTS AND DISCUSSION**

bioRxiv preprint doi: https://doi.org/10.1101/856864; this version posted November 27, 2019. The copyright holder for this preprint (which was not certified by peer review) is the author/funder, who has granted bioRxiv a license to display the preprint in perpetuity. It is made available under aCC-BY 4.0 International license.

90 **Elevated SPL activity has a modest effect on the *amp1* phenotype**

91 *amp1-1* (hereafter, *amp1*) mutants resemble plants with reduced *SPL* gene expression
92 in having an increased rate of leaf initiation, an increased number of rosette leaves, an
93 enlarged shoot apical meristem, and small, round rosette leaves that lack abaxial
94 trichomes (Fig. 1A-F) (Chaudhury et al., 1993; Huang et al., 2015; Telfer et al., 1997;
95 Yang et al., 2018). To determine if this phenotype is attributable to a reduction in *SPL*
96 activity, we introduced *35S::MIM156* — which de-represses *SPL* gene expression
97 (Franco-Zorrilla et al., 2007) — into *amp1*. *35S::MIM156* plants have a relatively slow
98 rate of leaf initiation, have enlarged and somewhat elongated rosette leaves, produce
99 abaxial trichomes unusually early in shoot development, and have a relatively small
100 SAM (Fig. 1A-F). *amp1; 35S::MIM156* plants had a vegetative phenotype intermediate
101 between that of the two parental genotypes, but which was more similar to *amp1* than to
102 *35S::MIM156*. The rosette leaves of *amp1; 35S::MIM156* were approximately the same
103 size as *amp1* leaves, but were similar in shape to *35S::MIM156* (Fig. 1A, B). *amp1*
104 plants rarely produced rosette leaves with abaxial trichomes (although abaxial trichome
105 production on cauline leaves was unaffected (Fig. S1)), whereas about 25% of *amp1;*
106 *35S::MIM156* produced rosette leaves with abaxial trichomes late in shoot development.
107 In contrast, all *35S::MIM156* plants produced rosette leaves with abaxial trichomes by
108 plastochron 3 (Fig. 1C). Similarly, the rate of leaf initiation in *amp1; 35S::MIM156* was
109 intermediate between that of *amp1* and *35S::MIM156*, but was closer to that of *amp1*
110 than *35S::MIM156* (Fig. 1D). The number of rosette leaves in *amp1; 35S::MIM156* was
111 also intermediate between these two genotypes, but was more similar to *amp1* than
112 *35S::MIM156* (Fig. 1E). Finally, the SAM of *amp1; 35S::MIM156* was more similar in

bioRxiv preprint doi: https://doi.org/10.1101/856864; this version posted November 27, 2019. The copyright holder for this preprint (which was not certified by peer review) is the author/funder, who has granted bioRxiv a license to display the preprint in perpetuity. It is made available under aCC-BY 4.0 International license.

113 size to *amp1* than to *35S::MIM156* (Fig. 1F). These results suggest that the phenotype
114 of *amp1* is not a consequence of repressed SPL activity, implying that *AMP1* acts either
115 downstream or in parallel to the miR156/*SPL* module. This conclusion is consistent with
116 the observation that vegetative development (Fig. 1C) and flowering time (Fig. 1G) are
117 dissociated in *amp1*.
118

119 **The phenotype of *amp1* is not attributable to a change in miR156/miR157 or *SPL***
120 **gene expression**

121 To explore the relationship between *AMP1* and the miR156/*SPL* module in more detail,
122 we examined the effect of *amp1* on the abundance of the miR156 and *SPL* transcripts.
123 qRT-PCR analysis of the shoot apices of plants grown in short days (SD) showed that
124 *amp1* had no significant effect on the level of miR156 or miR157 (Fig. 2A), or the
125 transcripts of three direct targets of these miRNAs: *SPL3*, *SPL9* and *SPL13* (Fig. 2B).
126 To test whether *amp1* affects *SPL* expression independent of miR156/miR157, we
127 measured the transcripts of these genes in *35S::MIM156* and *amp1; 35S:MIM156*
128 plants. As expected (He et al., 2018), all three *SPL* transcripts were significantly
129 elevated in *35S::MIM156.* All three transcripts were elevated to a much smaller extent in
130 *amp1; 35S:MIM156* (Fig. 2B). Together, these results suggest that *AMP1* may promote
131 *SPL* expression, but only in the absence of miR156/miR157.
132 We then examined the expression of these genes in successive rosette leaf
133 primordia (LP) of plants grown in SD. Because *amp1* initiates leaves more rapidly than
134 WT, LP were grouped according to the time of harvest rather than position on the shoot.
135 Both the level and rate of decline of miR156 were almost identical in WT and *amp1* (Fig.

bioRxiv preprint doi: https://doi.org/10.1101/856864; this version posted November 27, 2019. The copyright holder for this preprint (which was not certified by peer review) is the author/funder, who has granted bioRxiv a license to display the preprint in perpetuity. It is made available under aCC-BY 4.0 International license.

136 2C). miR157 was elevated in all LP, but declined at approximately the same rate as in
137 WT plants. *SPL9* and *SPL13* transcripts were also elevated in the LP of *amp1* relative to
138 WT (Fig. 2D), but these differences were relatively modest (two-fold or less) and not
139 statistically significant. Furthermore, the elevated expression of *SPL9* and *SPL13* is
140 inconsistent with the elevated level of miR157 and with the juvenilized phenotype of
141 *amp1*. Taken together, these data suggest that the vegetative phenotype of *amp1* is not
142 caused by increased expression of miR156/miR157 or decreased expression of *SPL*
143 genes. It is possible that *AMP1* regulates *SPL* expression independently of miR156
144 (Fig. 2B). However, the observation that *amp1* does not have a significant effect on
145 *SPL9* and *SPL13* expression at 20 DAP (Fig. 2D), when the levels of miR156 and
146 miR157 are very low (Fig. 2C), suggests that this is unlikely.
147 If *AMP1* does not regulate miR156 or *SPL* gene expression, perhaps it regulates
148 shared downstream targets. Consistent with this hypothesis, expression of the closely-
149 related *AP2-like* transcription factors *TOE1* and *TOE2* (which are targets of the SPL-
150 regulated miRNA, miR172) was consistently elevated in *amp1* (Fig. 2E). This effect is
151 not attributable to a change in the level of miR172, however, as the abundance of this
152 miRNA was not reduced in *amp1* (Fig. 2C). *TOE1* blocks the production of trichomes on
153 the abaxial side of the leaf by working in association with the abaxial specification
154 gene *KANAD1* (*KAN1*) to repress the transcription of *GLABRA1* (*GL1*) (Wang et al.,
155 2019; Xu et al., 2019). In WT plants, *GL1* expression increased dramatically between
156 13-14 DAP and 20 DAP, consistent with the increase in trichome production over this
157 period. *GL1* displayed a similar temporal pattern in *amp1*, but was almost completely
158 suppressed in the earliest LP and was considerably lower than WT in LP harvested at

bioRxiv preprint doi: https://doi.org/10.1101/856864; this version posted November 27, 2019. The copyright holder for this preprint (which was not certified by peer review) is the author/funder, who has granted bioRxiv a license to display the preprint in perpetuity. It is made available under aCC-BY 4.0 International license.

159 20 DAP (Fig. 2F). In contrast, the expression of *TRANSPARENT TESTA GLABRA1*
160 (*TTG1*) — which promotes trichome initiation via a distinct protein complex to *GL1*
161 (Pesch et al., 2015) — was not reduced in *amp1* (Fig. 2G). These results suggest that
162 *AMP1* promotes abaxial trichome formation via *GL1,* not *TTG1*, and that it acts as a
163 general activator of *GL1* expression, rather than a temporal regulator. They also support
164 the conclusion that *AMP1* regulates abaxial trichome production downstream of
165 miR156/*SPL*.
166
167 **The timing of vegetative phase change is regulated independently of leaf**
168 **initiation in *amp1***
169 The juvenilized phenotype of *amp1* was originally attributed to the increased rate of leaf
170 initiation in this mutant (Telfer et al., 1997). However, this interpretation is inconsistent
171 with more recent studies showing that pre-existing leaves promote the transition to the
172 adult vegetative phase by repressing miR156 (Yang et al., 2011; Yang et al., 2013; Yu
173 et al., 2013). To determine the basis of this discrepancy, we characterized the effect of
174 *CLAVATA3* (*CLV3*) and *CLV1* mutations on vegetative phase change. We chose these
175 mutations because they resemble *amp1* in having an enlarged SAM and an accelerated
176 rate of leaf initiation (Clark et al., 1995; Leyser and Furner, 1992).
177 Like *amp1* (Telfer et al., 1997), *clv3* and *clv1* produced smaller, rounder rosette
178 leaves, and more leaves without abaxial trichomes (Fig. 3A - C). This increase in the
179 number of juvenile-like leaves was not associated with a delay in the juvenile-to-adult
180 transition, however. Instead, *clv3* mutants produced leaves with abaxial trichomes one
181 day earlier than WT plants (Fig. 3D). To determine if the phenotype of *clv1* and *clv3* is

bioRxiv preprint doi: https://doi.org/10.1101/856864; this version posted November 27, 2019. The copyright holder for this preprint (which was not certified by peer review) is the author/funder, who has granted bioRxiv a license to display the preprint in perpetuity. It is made available under aCC-BY 4.0 International license.

182 dependent on miR156, we introduced the miR156 sponge, *35S::MIM156*, into these
183 mutants. This transgene was epistatic to *clv1* and *clv3* with respect to their effect on leaf
184 shape (Fig. 3A, B) and abaxial trichome production (Fig. 3C), suggesting that their effect
185 on these traits requires miR156.

186 We then examined the effect of *clv3* and *clv1* on the expression of miR156 and
187 its targets, *SPL9* and *SPL13*, in shoot apices (Fig. 3E) and LP (Fig. 3F). qRT-PCR
188 revealed that *clv1* and *clv3* have slightly reduced levels of miR156, although this
189 difference was only statistically significant in *clv3*. Consistent with the decreased
190 amount of miR156, *SPL9* and *SPL13* transcripts were slightly elevated in both the
191 mutants, although again this difference was only statistically significant in a few cases.
192 If these relatively small differences in miR156 and *SPL* gene expression are functionally
193 significant, they would be expected to promote the appearance of adult traits, not
194 repress the expression of these traits as is the case in *clv1* and *clv3*. To explore this
195 inconsistency, we examined the effect of *clv3* on the expression of a miR156-sensitive
196 and a miR156-resistant version of the *SPL9::SPL9-GUS* reporter (Xu et al., 2016).
197 There was no obvious difference in the expression of these reporters in the presence or
198 absence of *clv3* (Fig. 3G), supporting the conclusion that the effect of *clv3* on leaf
199 identity is not attributable to a change in the level of miR156 or its targets.

200 Instead, the effect of *clv3* and *clv1* on leaf identity is primarily attributable to their
201 effect on the rate of leaf initiation. Specifically, *clv3* and *clv1* appear to increase the
202 number of juvenile leaves by accelerating the rate of leaf production during the period
203 when miR156 levels are high. This conclusion is supported by the observation
204 that *35S::MIM156* is epistatic to these mutations with respect to their effect on leaf

bioRxiv preprint doi: https://doi.org/10.1101/856864; this version posted November 27, 2019. The copyright holder for this preprint (which was not certified by peer review) is the author/funder, who has granted bioRxiv a license to display the preprint in perpetuity. It is made available under aCC-BY 4.0 International license.

205 identity (Fig. 3A, B); i.e. miR156 is required for their leaf identity phenotypes. Consistent
206 with the evidence that leaves promote the juvenile-to-adult transition by repressing
207 miR156 (Yang et al., 2011; Yang et al., 2013; Yu et al., 2013), *clv3* and *clv1* have
208 slightly reduced levels of miR156 and slightly elevated levels of *SPL9* and *SPL13* (Fig.
209 3E, F). However, this relatively small effect is apparently insufficient to interfere with the
210 function of these genes in specifying juvenile leaf identity.
211 The increased number of juvenile leaves in *amp1* is also partly attributable to its
212 higher rate of leaf initiation (Telfer et al., 1997). However, *amp1* differs
213 from *clv3* and *clv1* in having a much more significant effect on leaf identity: *amp1* rarely
214 produces abaxial trichomes on rosette leaves, whereas *clv3* and *clv1* routinely do so. In
215 addition, the phenotype of *amp1* is less sensitive to a reduction in miR156 than the
216 phenotype of *clv3* and *clv1*; in general, *amp1, 35S::MIM156* plants more closely
217 resembled *amp1* than *35S::MIM156* (Fig. 1A-E). This observation, and the effect
218 of *amp1* on the expression of genes involved in abaxial trichome production (Fig. 2E, F),
219 suggest that AMP1 operates independently of miR156 to regulate genes involved in leaf
220 identity. A direct effect of AMP1 on leaf identity genes would explain why *amp1* has a
221 more severe vegetative phenotype than *clv3* and *clv1*, and why the phenotype
222 of *amp1* is relatively insensitive to changes in the level of miR156.
223

224 ***AMP1* is not universally required for translational repression**

225 Given the role of *AMP1* in translational repression (Li et al., 2013), it is possible that the
226 abundance of *SPL* transcripts in *amp1* (Fig. 2B, D) does not accurately reflect their
227 biological activity. To determine whether AMP1 is required for the post-transcriptional

bioRxiv preprint doi: https://doi.org/10.1101/856864; this version posted November 27, 2019. The copyright holder for this preprint (which was not certified by peer review) is the author/funder, who has granted bioRxiv a license to display the preprint in perpetuity. It is made available under aCC-BY 4.0 International license.

228 regulation of *SPL* genes, we first measured the amount of *SPL9* and *SPL13* transcript
229 cleavage in WT and *amp1* plants. Consistent with a previous study on miR156-
230 mediated cleavage (He et al., 2018), the rate of transcript cleavage for both *SPL9* and
231 *SPL13* declined during vegetative development in WT plants (Fig. 4A). This happened
232 at a slower rate in *amp1*, presumably in part due to the higher level of miR156 in the
233 *amp1* 13-14 DAP sample compared to WT (Fig. 2C) and the threshold-dependence of
234 miR156 activity (He et al., 2018). However, later in development, transcript cleavage in
235 *amp1* was similar to WT (Fig. 4A). This demonstrates that miR156 is functional in *amp1*
236 and confirms the observation that AMP1 is not required for transcriptional cleavage (Li
237 et al., 2013).

238 Although miR156 induces transcript cleavage, it represses the expression of its
239 targets primarily by promoting translational repression (He et al., 2018). To examine the
240 effect of *amp1* on this process, we crossed miR156-sensitive (sSPL9) and miR156-
241 resistant (rSPL9) GUS-reporter constructs of SPL9 into *amp1*. There was no obvious
242 difference in the staining intensity of these reporter proteins in WT and *amp1* (Fig. 4B).
243 To confirm this impression, we measured the staining intensity of the sSPL9-GUS
244 reporter spectrophotometrically in leaf primordia of WT and *amp1* harvested at a stage
245 when transcript cleavage was nearly equivalent in these genotypes (20 DAP (Fig. 4A)).
246 There was no significant difference in sSPL9 protein levels in these genotypes (Fig. 4C,
247 D). These results indicate that *amp1* has no effect on the activity of miR156, implying
248 that translational repression of *SPL9* occurs normally in *amp1*. To determine if miR156
249 is uniquely insensitive to *amp1*, we examined the effect of *amp1* on the expression of
250 MYB33, a transcription factor that also regulates shoot identity (Guo et al., 2017) and is

bioRxiv preprint doi: https://doi.org/10.1101/856864; this version posted November 27, 2019. The copyright holder for this preprint (which was not certified by peer review) is the author/funder, who has granted bioRxiv a license to display the preprint in perpetuity. It is made available under aCC-BY 4.0 International license.

251 translationally repressed by miR159 (Li et al., 2014). miR159-sensitive and miR159-
252 resistant versions of MYB33-GUS (Millar and Gubler, 2005) were crossed into *amp1*,
253 and WT and *amp1* plants were stained for GUS activity one week after germination, and
254 at flowering. MYB33-GUS was repressed in a miR159-dependent fashion in leaves and
255 floral organs of WT plants, and *amp1* had no obvious effect on this expression pattern
256 (Fig. 4E, F). Because *amp1* had no effect on the expression of sMYB33-GUS, it is
257 reasonable to assume that miR159-dependent translational repression occurs normally
258 in this mutant. We conclude from these results that *AMP1* is not universally required for
259 the translational repression of miRNA-targets.

260 Whether or not *AMP1* functions in translational repression may be a result of the
261 sub-cellular localization of the process. AMP1 has been shown to colocalize with the
262 key silencing component ARGONAUTE1 (AGO1) on the endoplasmic reticulum (ER)
263 (Li et al., 2013). However, AGO1 also localizes to processing bodies (p-bodies),
264 cytoplasmic foci of mRNA-ribonucleoprotein complexes that facilitate the sequestration
265 of mRNAs for translational silencing (reviewed in Chantarachot and Bailey-Serres,
266 2018). Loss of the p-body protein SUO leads to a reduction in the translational
267 repression of the miR156-target *SPL3* (Yang et al., 2012), suggesting that p-bodies are
268 also important sites of miRNA-mediated translational repression. Taken together, these
269 results are consistent with a model in which a) miRNA-mediated translational repression
270 occurs in distinct sub-cellular compartments in a sequence-specific manner and b)
271 unique sets of proteins contribute to this repression, depending on the compartment
272 (e.g. AMP1 on the ER, SUO in p-bodies). Whether the translational repression of
273 *MYB33* by miR159 occurs in p-bodies remains to be demonstrated.

bioRxiv preprint doi: https://doi.org/10.1101/856864; this version posted November 27, 2019. The copyright holder for this preprint (which was not certified by peer review) is the author/funder, who has granted bioRxiv a license to display the preprint in perpetuity. It is made available under aCC-BY 4.0 International license.

274 Support for this model comes from the finding that the microtubule severing-
275 enzyme KATANIN 1 is also required for translation repression (Brodersen et al., 2008).
276 What signals the cellular machinery uses to determine where to localize miRNA-target
277 pairs for translational repression is unclear. There appear to be no consistent
278 differences between the miRNA hairpin secondary structures and miRNA/miRNA*
279 duplexes of AMP1-dependent and AMP1-independent miRNAs (Fig. S2). Although it is
280 perhaps unlikely that any such signals would persist during miRNA processing. The
281 strength of target complementarity is known to affect silencing efficacy (Li et al., 2014),
282 and could also drive sub-cellular distribution, but there is also no trend in target
283 mismatch number between the AMP1-dependent/independent classes of miRNA (Table
284 S1). Given the overlapping expression domains of a number of these miRNAs
285 (reviewed in Fouracre and Poethig, 2016), it is unlikely that the site of translational
286 repression is developmentally regulated. At the cellular level, there is evidence to
287 suggest that miRNA sequences include signals that control the specificity of inter-
288 cellular mobility (Skopelitis et al., 2018). It will be fascinating to see if the same signaling
289 mechanisms determine the destination of miRNAs within cells.
290

291 **Materials and Methods**

292 **Plant material and growth conditions**

293 Col was used as the genetic background for all stocks. The following genetic lines have
294 been described previously: *amp1-1* (Chaudhury et al., 1993); *SPL9::sSPL9-GUS,*
295 *SPL9::rSPL9-GUS* (Xu et al., 2016); *35S::MIM156* (Fouracre and Poethig, 2019); *clv1-4*
296 (Clark et al., 1993); *MYB33::sMYB33-GUS, MYB33::rMYB33-GUS* (Millar and Gubler,

bioRxiv preprint doi: https://doi.org/10.1101/856864; this version posted November 27, 2019. The copyright holder for this preprint (which was not certified by peer review) is the author/funder, who has granted bioRxiv a license to display the preprint in perpetuity. It is made available under aCC-BY 4.0 International license.

297 2005). *clv3-10* (CS68823) was obtained from the Arabidopsis Biological Resource
298 Center (Ohio State University). Seeds were sown on fertilized Farfard #2 soil (Farfard)
299 and kept at 4°C for 3 days prior to transfer to a growth chamber, with the transfer day
300 counted as day 0 for plant age (0 DAP). Plant were grown at 22°C under a mix of both
301 white (USHIO F32T8/741) and red-enriched (Interlectric F32/T8/WS Gro-Lite)
302 fluorescent bulbs in either long day (16 hrs. light/8 hrs. dark; 80 µmol m^{-2} s^{-1}) or short
303 day (10 hrs light/14 hrs dark; 120 µmol m^{-2} s^{-1}) conditions.
304

305 **GUS staining**

306 Plants were fixed in 90% acetone on ice for 10 minutes and washed with GUS staining
307 buffer (5mM potassium ferricyanide and 5mM ferrocyanide in 0.1M PO_4 buffer) and
308 stained for between 8 hrs and overnight (depending on transgene strength) at 37°C in
309 2mM X-Gluc GUS staining buffer. For the quantification of GUS staining intensity,
310 ~1mm LP were harvested at 21 DAP, stained O/N and images of stained primordia
311 converted from RGB color mode to hue saturation brightness mode as previously
312 described (Béziat et al., 2017). A consistent position in the middle of the leaf lamina,
313 adjacent to the midvein, was used for measurement.
314

315 **Histology**

316 Shoot apices were cleared and imaged according to a described protocol (Chou et al.,
317 2016).
318

319 **RNA expression analyses**

bioRxiv preprint doi: https://doi.org/10.1101/856864; this version posted November 27, 2019. The copyright holder for this preprint (which was not certified by peer review) is the author/funder, who has granted bioRxiv a license to display the preprint in perpetuity. It is made available under aCC-BY 4.0 International license.

320 Tissue (either shoot apices with leaf primordia ≤1mm attached or isolated leaf primordia
321 0.5-1mm in size – as specified in the text) were ground in liquid nitrogen and total RNA
322 extracted using Trizol (Invitrogen) as per the manufacturer's instructions. RNA was
323 DNAse treated with RQ1 (Promgea) and 250ng-1µg of RNA was used for reverse
324 transcription using Superscript III (Invitrogen). Gene specific RT primers were used to
325 amplify miR156, miR157, miR172 and SnoR101 and a polyT primer for mRNA
326 amplification. Three-step qPCR of cDNA was carried out using SYBR-Green Master Mix
327 (Bimake). qPCR reactions were run in triplicate and an average taken. For analyses of
328 *amp1* shoot apices and *clv* mutants, separate RNA extractions of three biological
329 replicates were carried out. For analyses of *amp1* leaf primordia, three reverse-
330 transcription replicates from single RNA extractions were carried out for each sample (at
331 least 60 LP were pooled for each RNA extraction). 8 DAP samples were collected twice
332 - once as part of a biological replicate with 13-13 DAP and once as part of a biological
333 replicate with 20 DAP samples. Relative transcript levels were normalized to snoR101
334 (for miRNAs) and *ACT2* (*amp1* shoot apices, *clv* mutants) or *UBQ10* (*amp1* leaf
335 primordia) (for mRNAs) and expressed as a ratio of expression to WT (*amp1* shoot
336 apices, *clv* mutants) and WT 8 DAP (*amp1* leaf primordia) samples
337 For the quantification of transcript cleavage, a modified 5'RACE protocol was
338 followed as previously described (He et al., 2018). The data presented are the average
339 of three ratios from separate reverse transcription replicates (six in the case of *amp1* 8
340 DAP – three reverse transcription replicates from two biological replicates).
341 The qPCR primers used in this study are listed in Supplementary Table 2.
342

bioRxiv preprint doi: https://doi.org/10.1101/856864; this version posted November 27, 2019. The copyright holder for this preprint (which was not certified by peer review) is the author/funder, who has granted bioRxiv a license to display the preprint in perpetuity. It is made available under aCC-BY 4.0 International license.

343 **Statistical analyses**

344 A two-tailed Student's *t*-test was used to carry out pairwise comparisons between
345 different genotypes. For comparison of multiple samples, to decrease the chance of
346 false positives, a one-way ANOVA followed by a Tukey test was used for multi-way
347 comparisons. Statistical analyses were carried out in R (r-project.org) and Excel
348 (Microsoft).

349 For figures featuring boxplots, boxes display the IQR (boxes), median (lines), and
350 values beyond 1.5* IQR (whiskers); mean values are marked by a solid diamond (◆).

351

352

353 **Acknowledgements**

354 We thank Anthony Millar (Australian National University) for the kind gift of the MYB33-
355 GUS reporters, members of the Poethig lab for useful discussions and Melissa Morrison
356 for assistance with collecting phenotypic data.

357

358 **Competing interests**

359 No competing interests declared

360

361 **Funding**

362 This work was supported by the National Institutes of Health grant R01-GM51893 to R.
363 S.P.

364

365 **References**

bioRxiv preprint doi: https://doi.org/10.1101/856864; this version posted November 27, 2019. The copyright holder for this preprint (which was not certified by peer review) is the author/funder, who has granted bioRxiv a license to display the preprint in perpetuity. It is made available under aCC-BY 4.0 International license.

366 **Béziat, C., Kleine-Vehn, J. and Feraru, E.** (2017). Histochemical Staining of β-Glucuronidase
367 and Its Spatial Quantification. In *Plant Hormones: Methods and Protocols* (ed. Kleine-
368 Vehn, J. and Sauer, M.), pp. 73–80. New York, NY: Springer New York.

369 **Brodersen, P., Sakvarelidze-Achard, L., Bruun-Rasmussen, M., Dunoyer, P., Yamamoto,**
370 **Y. Y., Sieburth, L. and Voinnet, O.** (2008). Widespread translational inhibition by plant
371 miRNAs and siRNAs. *Science* **320**, 1185–1190.

372 **Chantarachot, T. and Bailey-Serres, J.** (2018). Polysomes, Stress Granules, and Processing
373 Bodies: A Dynamic Triumvirate Controlling Cytoplasmic mRNA Fate and Function.
374 *Plant Physiol.* **176**, 254–269.

375 **Chaudhury, A. M., Letham, S., Craig, S. and Dennis, E. S.** (1993). *amp1* - a mutant with high
376 cytokinin levels and altered embryonic pattern, faster vegetative growth, constitutive
377 photomorphogenesis and precocious flowering. *The Plant Journal* **4**, 907–916.

378 **Chou, H., Wang, H. and Berkowitz, G. A.** (2016). Shoot apical meristem size measurement.
379 *Bio-protocol* **6**, e2055.

380 **Chuck, G., Cigan, A. M., Saeteurn, K. and Hake, S.** (2007). The heterochronic maize mutant
381 *Corngrass1* results from overexpression of a tandem microRNA. *Nat Genet* **39**, 544–549.

382 **Clark, S. E., Running, M. P. and Meyerowitz, E. M.** (1993). *CLAVATA1*, a regulator of
383 meristem and flower development in *Arabidopsis*. *Development* **119**, 397–418.

384 **Clark, S. E., Running, M. P. and Meyerowitz, E. M.** (1995). *CLAVATA3* is a specific regulator
385 of shoot and floral meristem development affecting the same processes as *CLAVATA1*.
386 *Development* **121**, 2057–2067.

387 **Conway, L. J. and Poethig, R. S.** (1997). Mutations of *Arabidopsis thaliana* that transform
388 leaves into cotyledons. *Proc Natl Acad Sci USA* **94**, 10209–10214.

389 **Fouracre, J. P. and Poethig, R. S.** (2016). The role of small RNAs in vegetative shoot
390 development. *Curr Opin Plant Biol* **29**, 64–72.

391 **Fouracre, J. P. and Poethig, R. S.** (2019). Role for the shoot apical meristem in the
392 specification of juvenile leaf identity in *Arabidopsis*. *Proc Natl Acad Sci USA* **116**,
393 10168.

394 **Franco-Zorrilla, J. M., Valli, A., Todesco, M., Mateos, I., Puga, M. I., Rubio-Somoza, I.,**
395 **Leyva, A., Weigel, D., Garcia, J. A. and Paz-Ares, J.** (2007). Target mimicry provides
396 a new mechanism for regulation of microRNA activity. *Nat Genet* **39**, 1033–7.

397 **Guo, C., Xu, Y., Shi, M., Lai, Y., Wu, X., Wang, H., Zhu, Z., Poethig, R. S. and Wu, G.**
398 (2017). Repression of miR156 by miR159 regulates the timing of the juvenile-to-adult
399 transition in *Arabidopsis*. *Plant Cell* **29**, 1293–1304.

bioRxiv preprint doi: https://doi.org/10.1101/856864; this version posted November 27, 2019. The copyright holder for this preprint (which was not certified by peer review) is the author/funder, who has granted bioRxiv a license to display the preprint in perpetuity. It is made available under aCC-BY 4.0 International license.

400 **He, J., Xu, M., Willmann, M. R., McCormick, K., Hu, T., Yang, L., Starker, C. G., Voytas,**
401 **D. F., Meyers, B. C. and Poethig, R. S.** (2018). Threshold-dependent repression of *SPL*
402 gene expression by miR156/miR157 controls vegetative phase change in *Arabidopsis*
403 *thaliana*. *PLoS Genet.* **14**, e1007337.

404 **Helliwell, C. A., Chin-Atkins, A. N., Wilson, I. W., Chapple, R., Dennis, E. S. and**
405 **Chaudhury, A.** (2001). The *Arabidopsis AMP1* gene encodes a putative glutamate
406 carboxypeptidase. *Plant Cell* **13**, 2115–2125.

407 **Huang, W., Pitorre, D., Poretska, O., Marizzi, C., Winter, N., Poppenberger, B. and**
408 **Sieberer, T.** (2015). *ALTERED MERISTEM PROGRAM1* Suppresses Ectopic Stem Cell
409 Niche Formation in the Shoot Apical Meristem in a Largely Cytokinin-Independent
410 Manner. *Plant Physiol* **167**, 1471–1486.

411 **Huijser, P. and Schmid, M.** (2011). The control of developmental phase transitions in plants.
412 *Development* **138**, 4117–4129.

413 **Leichty, A. R. and Poethig, R. S.** (2019). Development and evolution of age-dependent
414 defenses in ant-acacias. *Proc Natl Acad Sci USA* **116**, 15596.

415 **Leyser, H. M. O. and Furner, I. J.** (1992). Characterization of three shoot apical meristem
416 mutants of *Arabidopsis thaliana*. *Development* **116**, 397–403.

417 **Li, S., Liu, L., Zhuang, X., Yu, Y., Liu, X., Cui, X., Ji, L., Pan, Z., Cao, X., Mo, B., et al.**
418 (2013). MicroRNAs inhibit the translation of target mRNAs on the endoplasmic
419 reticulum in *Arabidopsis*. *Cell* **153**, 562–74.

420 **Li, J., Reichel, M. and Millar, A. A.** (2014). Determinants beyond both complementarity and
421 cleavage govern microR159 efficacy in *Arabidopsis*. *PLoS Genet* **10**, e1004232.

422 **Millar, A. A. and Gubler, F.** (2005). The Arabidopsis GAMYB-like genes, *MYB33* and
423 *MYB65*, are microRNA-regulated genes that redundantly facilitate anther development.
424 *Plant Cell* **17**, 705–21.

425 **Pesch, M., Schultheiß, I., Klopffleisch, K., Uhrig, J. F., Koegl, M., Clemen, C. S., Simon, R.,**
426 **Weidtkamp-Peters, S. and Hülskamp, M.** (2015). TRANSPARENT TESTA
427 GLABRA1 and GLABRA1 Compete for Binding to GLABRA3 in *Arabidopsis*. *Plant*
428 *Physiol.* **168**, 584–597.

429 **Poethig, R. S.** (2013). Vegetative phase change and shoot maturation in plants. *Curr. Top. Dev.*
430 *Biol.* **105**, 125–52.

431 **Riese, M., Zobell, O., Saedler, H. and Huijser, P.** (2008). SBP-domain transcription factors as
432 possible effectors of cryptochrome-mediated blue light signalling in the moss
433 *Physcomitrella patens*. *Planta* **227**, 505–15.

bioRxiv preprint doi: https://doi.org/10.1101/856864; this version posted November 27, 2019. The copyright holder for this preprint (which was not certified by peer review) is the author/funder, who has granted bioRxiv a license to display the preprint in perpetuity. It is made available under aCC-BY 4.0 International license.

434 **Skopelitis, D. S., Hill, K., Klesen, S., Marco, C. F., von Born, P., Chitwood, D. H. and**
435 **Timmermans, M. C. P.** (2018). Gating of miRNA movement at defined cell-cell
436 interfaces governs their impact as positional signals. *Nat. Commun.* **9**, 3107.

437 **Telfer, A., Bollman, K. M. and Poethig, R. S.** (1997). Phase change and the regulation of
438 trichome distribution in *Arabidopsis thaliana*. *Development* **124**, 645–654.

439 **Wang, J. W., Park, M. Y., Wang, L. J., Koo, Y., Chen, X. Y., Weigel, D. and Poethig, R. S.**
440 (2011). miRNA control of vegetative phase change in trees. *PLoS Genet* **7**, e1002012.

441 **Wang, L., Zhou, C.-M., Mai, Y.-X., Li, L.-Z., Gao, J., Shang, G.-D., Lian, H., Han, L.,**
442 **Zhang, T.-Q., Tang, H.-B., et al.** (2019). A spatiotemporally regulated transcriptional
443 complex underlies heteroblastic development of leaf hairs in Arabidopsis thaliana. *The*
444 *EMBO Journal* **38**, e100063.

445 **Wu, G. and Poethig, R. S.** (2006). Temporal regulation of shoot development in *Arabidopsis*
446 *thaliana* by miR156 and its target *SPL3*. *Development* **133**, 3539–47.

447 **Wu, G., Park, M. Y., Conway, S. R., Wang, J. W., Weigel, D. and Poethig, R. S.** (2009). The
448 sequential action of miR156 and miR172 regulates developmental timing in *Arabidopsis*.
449 *Cell* **138**, 750–9.

450 **Xu, M., Hu, T., Zhao, J., Park, M. Y., Earley, K. W., Wu, G., Yang, L. and Poethig, R. S.**
451 (2016). Developmental functions of miR156-regulated *SQUAMOSA PROMOTER*
452 *BINDING PROTEIN-LIKE* (*SPL*) genes in *Arabidopsis thaliana*. *PLoS Genet.* **12**,
453 e1006263.

454 **Xu, Y., Qian, Z., Zhou, B. and Wu, G.** (2019). Age-dependent heteroblastic development of
455 leaf hairs in Arabidopsis. *New Phytologist* **224**, 741–748.

456 **Yang, L., Conway, S. R. and Poethig, R. S.** (2011). Vegetative phase change is mediated by a
457 leaf-derived signal that represses the transcription of miR156. *Development* **138**, 245–9.

458 **Yang, L., Wu, G. and Poethig, R. S.** (2012). Mutations in the GW-repeat protein SUO reveal a
459 developmental function for microRNA-mediated translational repression in Arabidopsis.
460 *Proc Natl Acad Sci USA* **109**, 315–320.

461 **Yang, L., Xu, M., Koo, Y., He, J. and Poethig, R. S.** (2013). Sugar promotes vegetative phase
462 change in *Arabidopsis thaliana* by repressing the expression of *MIR156A* and *MIR156C*.
463 *Elife* **2**, e00260.

464 **Yang, S., Poretska, O. and Sieberer, T.** (2018). ALTERED MERISTEM PROGRAM1
465 Restricts Shoot Meristem Proliferation and Regeneration by Limiting HD-ZIP III-
466 Mediated Expression of RAP2.6L. *Plant Physiol.* **177**, 1580–1594.

467 **Yu, S., Cao, L., Zhou, C. M., Zhang, T. Q., Lian, H., Sun, Y., Wu, J. Q., Huang, J. R.,**
468 **Wang, G. D. and Wang, J. W.** (2013). Sugar is an endogenous cue for juvenile-to-adult
469 phase transition in plants. *Elife* **2**, e00269.

bioRxiv preprint doi: https://doi.org/10.1101/856864; this version posted November 27, 2019. The copyright holder for this preprint (which was not certified by peer review) is the author/funder, who has granted bioRxiv a license to display the preprint in perpetuity. It is made available under aCC-BY 4.0 International license.

470

471 **Figure Legends**

472 **Fig. 1. Elevated *SPL* gene activity only partially suppresses the *amp1* phenotype.**
473 (A) Photographs of plants taken at 16 DAP, scale bar: 5mm. (B) Silhouettes of
474 heteroblastic series of rosette leaves for lines shown in (A). (C) Percentage of individual
475 plants that produced at least one rosette leaf with abaxial trichomes ($n \geq 18$). (D) Leaf
476 emergence was scored when leaves became visible without manipulation of the rosette,
477 error bars represent the SEM ($n \geq 18$). (E, F, G) Statistically distinct genotypes were
478 identified by one-way ANOVA with *post hoc* Tukey multiple comparison test (letters
479 indicate statistically distinct groups; $p < 0.05$; sample sizes are shown in the figure).
480 Images and measurements in (F) are of SAMs of plants harvested at 5 DAP captured
481 using DIC microscopy, scale bar: 100μM. All phenotypic analyses were carried out in
482 LD conditions.

483 **Fig. 2. The *amp1* phenotype is not associated with repressed *SPL* activity.** qRT-
484 PCR analyses of gene expression. (A, B) Shoot apices with leaf primordia ≥ 1mm
485 removed at 8 DAP. (C - G) Isolated leaf primordia (LP) 0.5-1mm in size. 8 DAP = LP1-2;
486 13-14 DAP = LP 4-5 (*amp1* LP were harvested at 13 DAP, WT LP at 14 DAP); 20 DAP
487 = WT LP9-10, *amp1* LP14-16. Error bars represent the SEM. All plants were grown in
488 SD conditions. Asterisks represent significant differences between genotypes calculated
489 by two-tailed *t*-test ($p < 0.05$ = *; $p < 0.01$ = **; $p < 0.001$ = ***).

490 **Fig. 3. Enhanced *clv* juvenility is a consequence of an increased rate of leaf**
491 **initiation, rather than repressed *SPL* gene activity.** (A) Photographs were taken at

bioRxiv preprint doi: https://doi.org/10.1101/856864; this version posted November 27, 2019. The copyright holder for this preprint (which was not certified by peer review) is the author/funder, who has granted bioRxiv a license to display the preprint in perpetuity. It is made available under aCC-BY 4.0 International license.

492 21 DAP, scale bar: 5mm. (B) Silhouettes of heteroblastic series of rosette leaves for
493 lines shown in (A). (C) Statistically distinct genotypes were identified by one-way
494 ANOVA with *post hoc* Tukey multiple comparison test (letters indicate statistically
495 distinct groups; $p < 0.05$; sample sizes are shown in the figure). (D) Leaf emergence
496 was scored when leaves became visible without manipulation of the rosette, the dashed
497 line indicates the first leaf to produce abaxial trichomes, error bars represent the SEM (n
498 ≥ 23). (E, F) qRT-PCR analyses of gene expression of (E) shoot apices with leaf
499 primordia ≥ 1mm removed at 10 DAP and (F) isolated LP1&2 0.5-1mm in size. Asterisks
500 represent significant differences between WT vs *clv3* or WT vs *clv1*. Significance was
501 calculated by two-tailed *t*-test ($p < 0.05$). (G) GUS staining of miR156-sensitive and
502 miR156-resistant SPL-GUS reporter constructs at 14 DAP. Phenotypic analyses were
503 carried out in LD conditions (A-D), gene expression analyses were carried out in SD
504 conditions (E-G).

505 **Fig. 4. miRNA-regulated SPL9 and MYB33 proteins accumulate normally in *amp1*.**
506 (A) The relative abundance of uncleaved/cleaved transcripts, normalized to WT 8 DAP.
507 See Fig. 2B legend for details of samples. (B) GUS staining of miR156-sensitive and
508 miR156-resistant SPL-GUS reporter constructs at 21 DAP. (C, D) Quantification of
509 sSPL9-GUS protein levels by image analysis. RGB color mode ((C), top panels), hue
510 saturation brightness mode ((C), bottom panels). Red squares indicate where signal
511 intensity was measured, each dot represents an individual primordia (D). (E, F) GUS
512 staining of miR159-sensitive and miR159-resistant MYB33-GUS reporter constructs in 7
513 DAP seedlings (E) and flowers (F). Scale bars: (B) 5mm, (C) 200μM, (E, F) 1mm.

bioRxiv preprint doi: https://doi.org/10.1101/856864; this version posted November 27, 2019. The copyright holder for this preprint (which was not certified by peer review) is the author/funder, who has granted bioRxiv a license to display the preprint in perpetuity. It is made available under aCC-BY 4.0 International license.

514

515 **Supplementary Fig. 1. *amp1* cauline leaves produce abaxial trichomes.** Scale bar:
516 2mm

517 **Supplementary Fig. 2 Predicted hairpin structures for miRNAs that are *AMP1*-**
518 **dependent and independent for translational repression.** *AMP1*-independent (this
519 study) – miR156, miR157, miR159; *AMP1*-dependent (Li et al., 2013) – miR164,
520 miR165, miR166 and miR398. Representative functional members of miRNA families
521 are displayed. Stem-loop sequences were downloaded from miRBase
522 (www.mirbase.org) and hairpin structures predicted using the default settings on
523 RNAfold (http://rna.tbi.univie.ac.at/). Minimum free-energy models of hairpins are
524 shown, color coded for base pair probability. Black lines are drawn alongside mature
525 miRNA sequences.

526

527

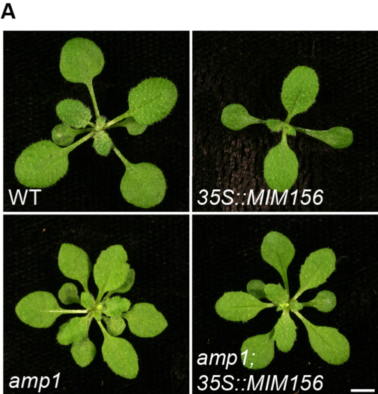
A
WT
35S::MIM156
amp1
amp1;
35S::MIM156

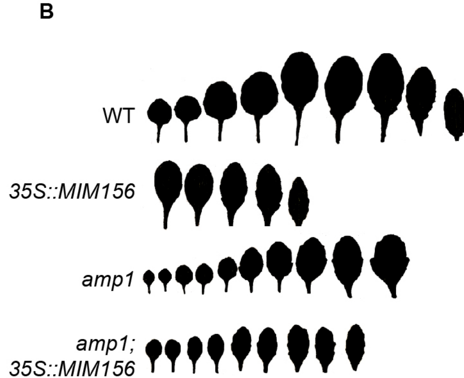
B
WT
35S::MIM156
amp1
amp1;
35S::MIM156

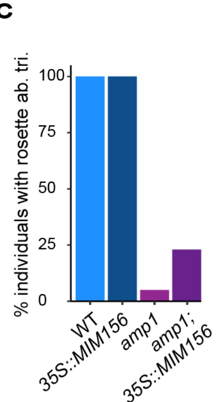
C
% individuals with rosette ab. tri.
0
25
50
75
100
WT
35S::MIM156
amp1
amp1;
35S::MIM156

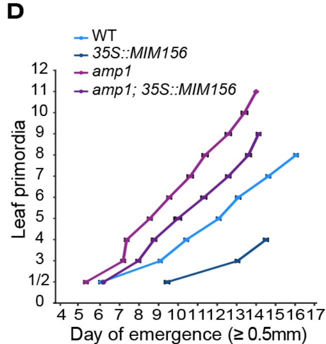
D
WT
35S::MIM156
amp1
amp1; 35S::MIM156
Leaf primordia
Day of emergence (≥ 0.5mm)

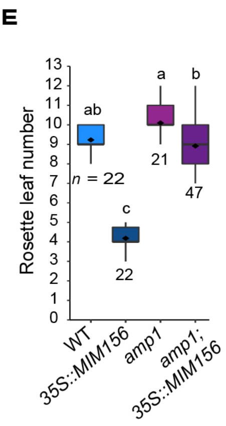
E
Rosette leaf number
ab
a
b
c
n = 22
21
47
22
WT
35S::MIM156
amp1
amp1;
35S::MIM156

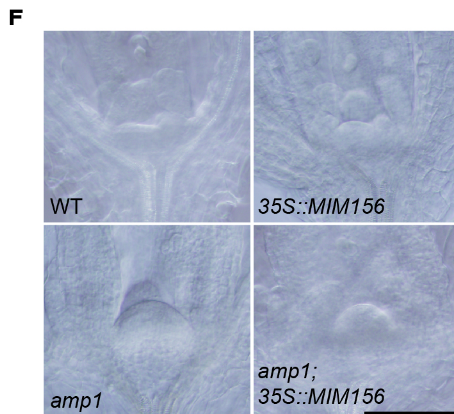
F
WT
35S::MIM156
amp1
amp1;
35S::MIM156

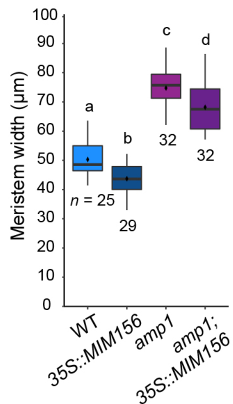
Meristem width (µm)
a
b
c
d
n = 25
29
32
32
WT
35S::MIM156
amp1
amp1;
35S::MIM156

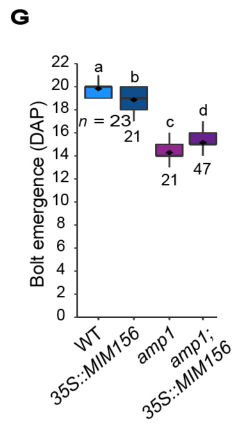
G
Bolt emergence (DAP)
a
b
c
d
n = 23
21
21
47
WT
35S::MIM156
amp1
amp1;
35S::MIM156

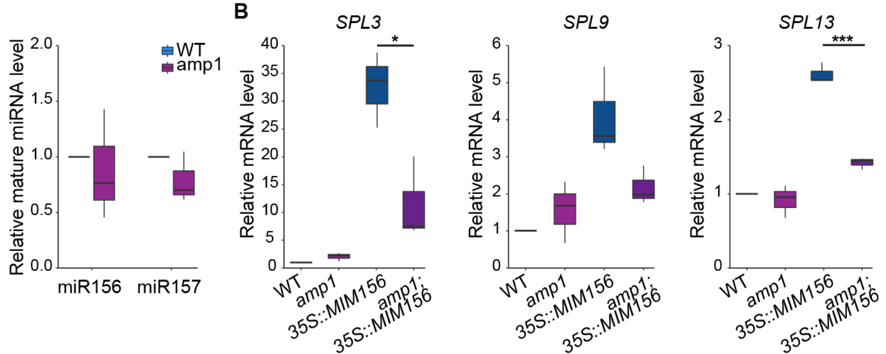
A
Relative mature miRNA level
2.0
1.5
1.0
0.5
0.0
WT
amp1
miR156
miR157
B
SPL3
SPL9
SPL13
Relative mRNA level
*
***
WT
amp1
35S::MIM156
amp1;
35S::MIM156

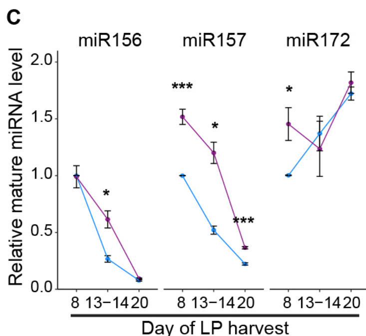
C
miR156
miR157
miR172
Relative mature miRNA level
*
***
*
***
*
8
13−14
20
Day of LP harvest

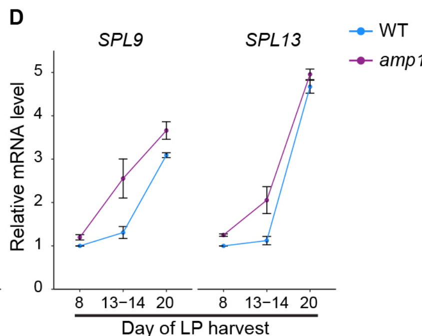
D
SPL9
SPL13
Relative mRNA level
WT
amp1
8
13−14
20
Day of LP harvest

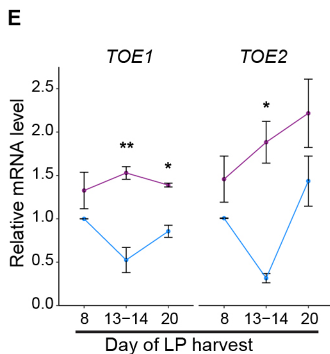
E
TOE1
TOE2
Relative mRNA level
**
*
*
8
13−14
20
Day of LP harvest

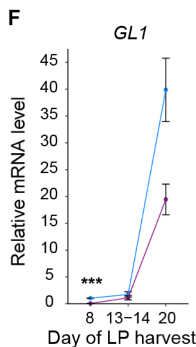
F
GL1
Relative mRNA level
***
8
13−14
20
Day of LP harvest

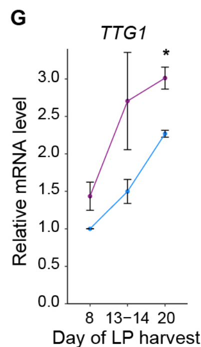
G
TTG1
Relative mRNA level
*
8
13−14
20
Day of LP harvest

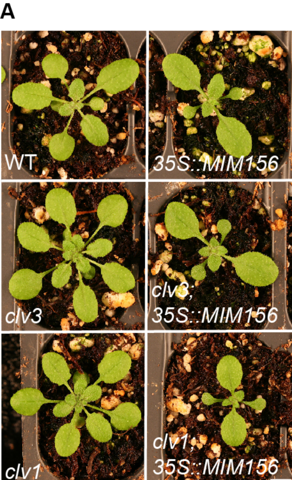
A
WT
35S::MIM156
clv3
clv3;
35S::MIM156
clv1
clv1;
35S::MIM156

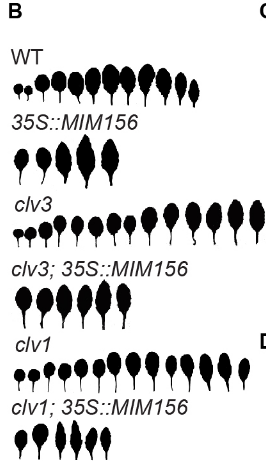
B
WT
35S::MIM156
clv3
clv3; 35S::MIM156
clv1
clv1; 35S::MIM156

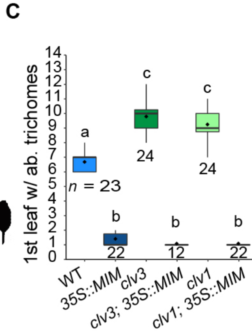
C
1st leaf w/ ab. trichomes
a
b
c
b
c
b
n = 23
22
24
12
24
22
WT
35S::MIM
clv3
clv3; 35S::MIM
clv1
clv1; 35S::MIM

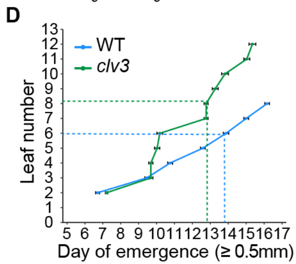
D
WT
clv3
Leaf number
Day of emergence (≥ 0.5mm)

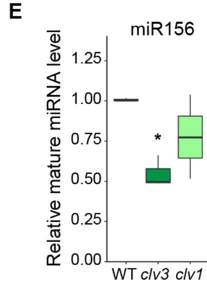
E
miR156
Relative mature miRNA level
WT
clv3
clv1

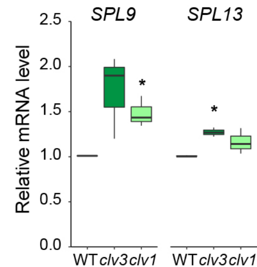
SPL9
SPL13
Relative mRNA level
WT
clv3
clv1

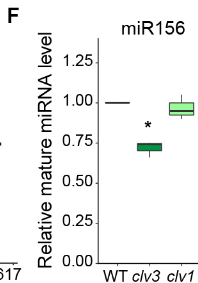
F
miR156
Relative mature miRNA level
WT
clv3
clv1

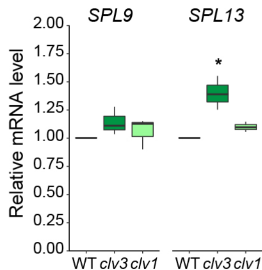
SPL9
SPL13
Relative mRNA level
WT
clv3
clv1

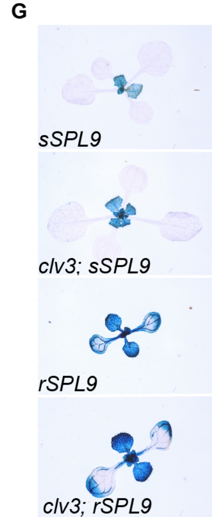
G
sSPL9
clv3; sSPL9
rSPL9
clv3; rSPL9

A
WT
amp1
Uncleaved/cleaved relative abundance
0
1
2
3
4
5
6
SPL9
SPL13
8
13−14
20
8
13−14
20
Day of LP harvest

B
sSPL9
rSPL9
amp1; sSPL9
amp1; rSPL9